Analysis on data storage area of NiO-ReRAM with secondary electron image

K. Kinoshita[a)]
Department of Information and Electronics, Graduate School of Engineering, Tottori University, Tottori 680-8552, Japan; and Tottori University Electronic Display Research Center, Tottori 680-0941, Japan

T. Makino, T. Yoda, and K. Dobashi
Department of Information and Electronics, Graduate School of Engineering, Tottori University, Tottori 680-8552, Japan

S. Kishida
Department of Information and Electronics, Graduate School of Engineering, Tottori University, Tottori 680-8552, Japan; and Tottori University Electronic Display Research Center, Tottori 680-0941, Japan

(Received 24 June 2010; accepted 24 September 2010)

Both low and high resistance states (which were written by voltage application in a local region of NiO/Pt films using conducting atomic force microscopy [C-AFM]) were observed with scanning electron microscopy (SEM) and electron probe microanalysis (EPMA). The writing regions are distinguishable as dark areas in a secondary electron image and thus can be specified without using a complicated sample fabrication process to narrow down the writing regions such as the photolithography technique. In addition, the writing regions were analyzed using energy-dispersive x-ray spectroscopy (EDS) mapping. No difference between the inside and outside of the writing regions is observed for all the mapped elements including C and Rh. Here, C and Rh are the most probable candidates for contamination that affect the secondary electron image. Therefore, our results suggested that the observed change in the contrast of the secondary electron image is related to the intrinsic change in the electronic state of the NiO film and a secondary electron yield is correlated to the physical properties of the film.

I. INTRODUCTION

In recent years advances have been made in the research and development of resistive random-access memory (ReRAM) that uses voltage-induced resistive change in transition metal oxides (TMOs) as memory media. ReRAM is a candidate for a substitution for Flash memory, which is facing a microfabrication limit in the near future. Furthermore, a development of a nonvolatile and high-density universal memory with fast switching and high switching endurance is expected in the future. However, the optimization of the performance and the establishment of reliability have been prevented by the fact that the switching mechanism of ReRAM has not yet been clarified. Therefore, the elucidation of the switching mechanism is urgently required.

ReRAM has a simple structure of a top electrode (TE)/TMO/a bottom electrode (BE). Memory effect develops after a forming process, and it becomes possible to cause a set, which is a resistive switching from a high resistance state (HRS) to a low resistance state (LRS), and a reset, which is a resistive switching from the LRS to the HRS, alternately. Here, the forming is a phenomenon, which is similar to a soft breakdown, and a conductive path called a filament is formed after it. Resistive switching is thought to take place in the filament.[1–4] The reason why the elucidation of resistive switching mechanism is hindered is attributed to the difficulty in applying conventional analytical methods to the resistance switching region because the filament is covered with electrodes and the radius of the filament is very small.[5,6]

Recently, it was demonstrated that both the LRS and the HRS can be written over an arbitrary area by applying direct-current (DC) bias voltage, V_{bias}, directly to NiO films using conducting atomic force microscopy (C-AFM).[7,8] The resistance writing region consists of the aggregation of filaments and can be regarded as one filament with a large radius. Therefore, this technique can provide the filament with an arbitrary radius without TE, which allows application of conventional analytical methods and might be a breakthrough for the switching mechanism elucidation.

In this paper, the LRS and the HRS with the large area of $20 \times 20\ \mu m^2$ were written in a NiO/Pt film by voltage application using C-AFM. Taking advantage of the large size of the target area, the writing regions were analyzed using scanning electron microscopy (SEM), electron microprobe (EPMA), and energy-dispersive x-ray spectroscopy

a)Address all correspondence to this author.
e-mail: Kinoshita@ele.tottori-u.ac.jp
DOI: 10.1557/jmr.2010.57

 © Materials Research Society 2011

https://doi.org/10.1557/jmr.2010.57 Published online by Cambridge University Press

(EDS) for the elucidation of a physical property of the filament.

II. EXPERIMENTAL

A 60 nm NiO film was deposited on a Pt(100 nm)/Ti (20 nm)/SiO_2(100 nm)/Si(625 μm) substrate by using DC reactive magnetron sputtering at 380 °C in the mixture gas of Ar and O_2 gases (Ar + O_2 gas), and a NiO/Pt/Ti/SiO_2 (NiO/Pt) structure was obtained. Here, the SiO_2/Si structure was formed by thermal oxidation of Si wafer and a Ni metal with the purity of 99.99% was used as a sputtering target. During the deposition, the pressure of Ar + O_2 gas was retained at 0.5 Pa (Ar: O_2 = 0.45 Pa: 0.05 Pa).

For the C-AFM measurements, we used a commercial AFM (SPI3800N/SPA400, Seiko). A Rh-coated Si tip with the point diameter of 100 nm [SI-DF3-R(100 nm), Seiko] was grounded, and the V_{bias} was applied to the BE. HRS or LRS was written in the central 20 × 20 μm^2 area by scanning the tip under V_{bias} of −7 V or +7 V, respectively. Subsequently, the 22 × 22 μm^2 area containing the writing region was scanned with a sensing voltage of +1 V. The HRS was written with a negative bias, whereas LRS with a positive bias is reported in Ref. 7. The scanning frequency was 1 Hz, and the data density was 256 × 256. All the C-AFM measurements were performed in the atmosphere.

Analyses with EPMA and SEM on the regions where the HRS and the LRS were written were conducted. EDS mapping analysis on areas containing these writing regions were also performed.

III. RESULTS AND DISCUSSION

A. Resistance states written by using C-AFM

Figures 1(a) and 1(b) show current–voltage (*I–V*) characteristics of AFM-tip/NiO/Pt structures measured by positioning the tip at the arbitrary selected point, and applying V_{bias} of +7 V and −7 V, respectively, where voltage steps were 7 mV and a hold time, a delay time, and a voltage sweep rate were 1 ms, 0 s, and 0.7 V/s, respectively. Here, NiO is in the initial state in both Figs. 1(a) and 1(b). It was confirmed that HRS was written by the application of negative V_{bias}, whereas LRS was written by the application of positive V_{bias}, which is consistent with Ref. 7. This effect is hard to interpret as an anodization of the NiO surface, which is caused by the electrolysis of water between the NiO surface and the AFM-tip,[9] since reset occurs by applying a negative V_{bias} to the bottom electrode, which is the opposite bias polarity needed for the anodization to occur.

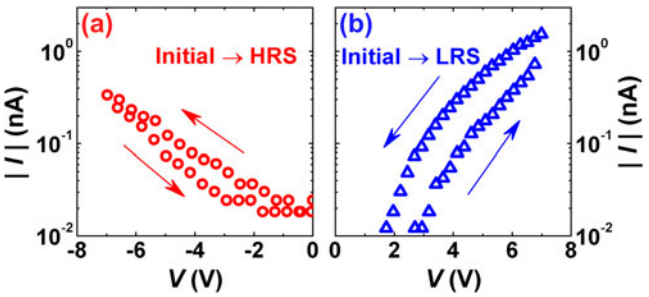


FIG. 1. *I–V* characteristics measured with C-AFM by application of V_{bias} of (a) +7 V and (b) −7 V, respectively.

Figures 2(a) and 2(b) show current images before and after performing C-AFM writing under V_{bias} of +7 V, respectively. On the other hand, Figs. 2(c) and 2(d) show current images before and after performing C-AFM writing under V_{bias} of −7 V, respectively. All the current images shown in Figs. 2(a)–2(d) were measured with a scanning frequency of 1 Hz. The bright contrast regions in the current image correspond to the LRS and the dark contrast regions to the HRS. Averaged currents at the sensing voltage of 0.1 V for the initial state, HRS, and LRS were 12.1, 0.1, and 82.6 pA, respectively.

B. SEM and EPMA analyses

Figure 3(a) shows the locations of four 20 × 20 μm^2 regions on the NiO film to which resistance states were written by using C-AFM. Resistance states of the regions (1), (2), (3), and (4) were written by scanning the AFM tip under V_{bias} of +7 V, −7 V, +5 V, and −5 V, respectively. Regions (1) and (3) were written to the LRS, whereas regions (2) and (4) were written to the HRS. That is, the resistance decreased by application of positive bias, whereas increased by negative bias, as described previously. The scratch in the figure was introduced by a diamond-point pencil to support finding out the same place containing these regions by EPMA and SEM.

Figures 3(b), 3(c), and 3(d) represent secondary electron (SE), composition (COMP), and topographic (TOPO) images of the NiO film containing all the regions (1)–(4), respectively. Here, COMP and TOPO images are obtained by a primary electron emission, which is sensitive to both the composition and surface morphology of the sample. Dark regions in Fig. 3(b), where a secondary electron yield is low compared with the other region, correspond to the regions (1)–(4), whereas no difference in the contrast from the surrounding region is observed in the corresponding region in Figs. 3(c) and 3(d). In addition, the writing region in the SE image becomes darker with increasing the amplitude of writing voltage.

Figures 4(a) and 4(b) show SE images before and after C-AFM writing (not the same position). Tetrahedral grain structures are observed on the surface, showing the (111) orientation of the NiO film. No remarkable change in both sizes and shapes of NiO grains were observed. No damage caused by the writing current was also confirmed.

Figure 5 shows applied bias and scanning frequency dependences of a SE image for writing regions. In Fig. 5,

https://doi.org/10.1557/jmr.2010.57 Published online by Cambridge University Press

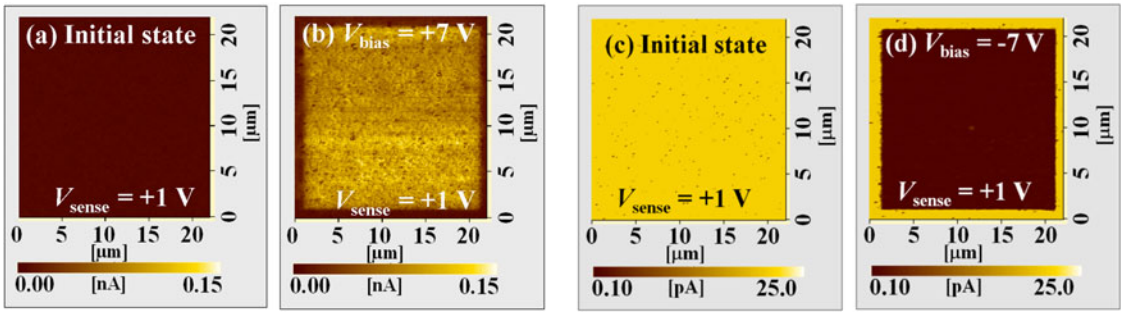


FIG. 2. Current images (a) before and (b) after C-AFM writing by scanning under V_{bias} of +7 V. Current images (c) before and (d) after C-AFM writing by scanning under V_{bias} of −7 V.

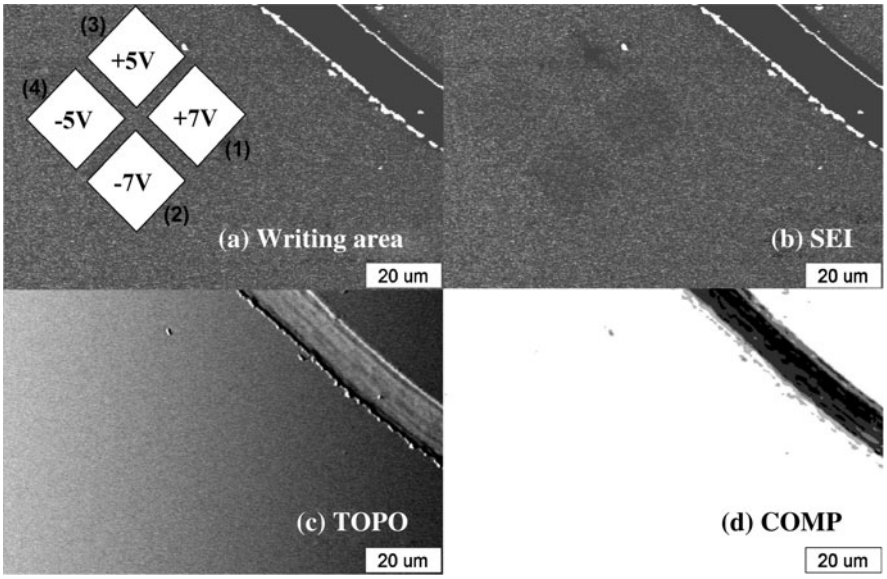


FIG. 3. (a) Location of regions (1)–(4) written by scanning under V_{bias} of +7, −7, +5, and −5 V using C-AFM, respectively. (b) SE, (c) TOPO, and (d) COMP images of the NiO film in which regions (1)–(4) are included.

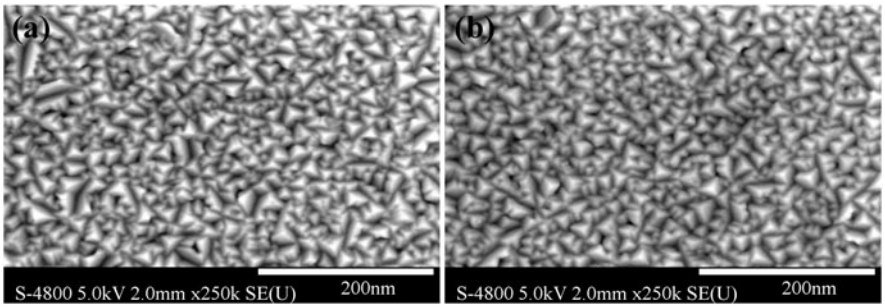


FIG. 4. Secondary electron images before and after C-AFM writing under V_{bias} of +7 V with a scanning frequency of 0.2 Hz.

regions (1)–(3) were written to the LRS and regions (4)–(6) were written to the HRS under the writing conditions shown in Table I. The higher the applied bias becomes and/or the lower the scanning frequency becomes, the darker the SE image of the writing regions becomes. Therefore, a darker SE image is obtained by applying V_{bias} with larger amplitude for a longer duration to the unit area.

C. EDS mapping analysis

As possible main factors that cause the change in the contrast of a SE image by the application of V_{bias} using C-AFM, the following three factors can be pointed out: (i) The change in the surface morphology has been caused. (ii) Removal/adhesion of contaminations from/to the surface of the NiO film has been caused. (iii) An intrinsic

https://doi.org/10.1557/jmr.2010.57 Published online by Cambridge University Press

change in electronic state of NiO has been caused. Since no remarkable change in the surface morphology of the sample by the application of C-AFM writing was observed as shown in Fig. 4, which denied the factor (i), the possibility of the factor (ii) is discussed below.

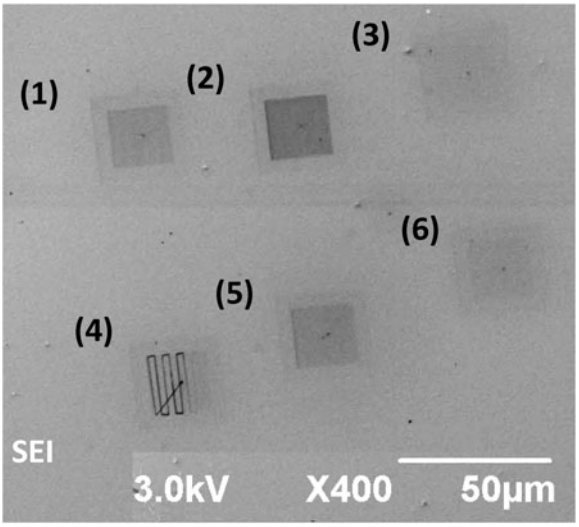


FIG. 5. Secondary electron image after C-AFM writing for regions (1)–(6) under the conditions shown in Table I.

TABLE I. Conditions under which regions (1)–(6) in Figs. 5 and 6(a) were written to the HRS or the LRS by using C-AFM.

Writing regions	Writing voltage V [V]	Frequency ν [Hz]
(1)	+9	1
(2)	+9	0.2
(3)	+5	1
(4)	−9	1
(5)	−9	0.2
(6)	−5	1

Elements for which EDS mapping analysis were conducted were selected as follows. Hilleret et al. reported that secondary electron yield of an air exposed ZnO film decreased after annealing the film.[10] This is due to a removal of airborne carbonaceous contamination layer formed on the surface of the sample by the annealing process. Analogously, also in the present study, the removal of carbonaceous contamination might be caused by Joule heating generated during C-AFM writing. Therefore, C was selected as a mapping element. In addition, Rh with which the AFM tip is coated might adhere to the scanned area. By adding the constituent elements of the sample to C and Rh, EDS mapping analyses were performed on C, Rh, Ni, O, and Pt.

Figure 6(a), which is the same figure as Fig. 5, shows the SE image after the C-AFM writing. The square regions surrounded by dotted lines correspond to the writing regions that were written under the conditions shown in Table I. Figures 6(b)–6(f) show results of EDS mapping measurements for Rh, C, O, Ni, and Pt, respectively. Here, the square regions surrounded by dotted lines in Figs. 6(b)–6(f) correspond to the writing regions in Fig. 6(a), respectively. The acceleration voltage was 3.0 kV. Energies of C Kα, O Kα, Ni Lα, Pt Mα, and Rh Lα lines are 0.277, 0.525, 0.851, 2.050, and 2.696 eV, respectively.

No difference of the intensity distribution in the EDS mappings between inside and outside of the writing regions was observed for all the mapped elements, suggesting the exclusion of the factor (ii). Therefore, as a reason why the SE image becomes dark by the voltage application, it was suggested that the change in the

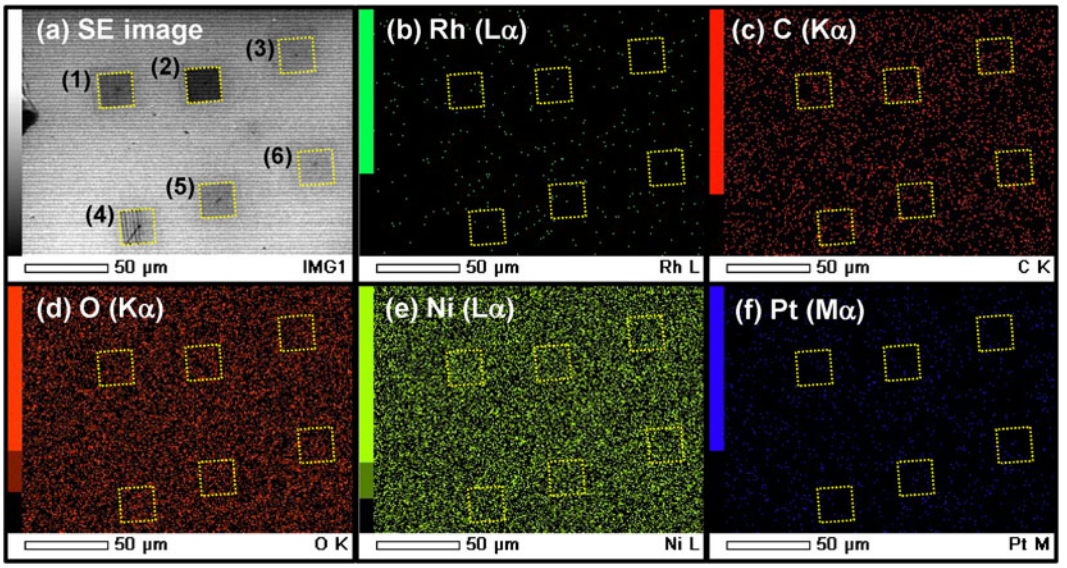


FIG. 6. (a) Secondary electron image after writing under the conditions shown in Table I, which is the same as Fig. 5. EDS mapping results for (b) Rh, (c) C, (d) O, (e) Ni, and (f) Pt.

https://doi.org/10.1557/jmr.2010.57 Published online by Cambridge University Press

electric conductivity of NiO affected the secondary electron yield.

It has been widely received that the resistance change effect observed in transition metal oxides is caused by the migration of oxygen ions,[2,7,11] which introduces or repairs oxygen vacancies depending on the applied bias condition. It has also been received that the LRS is formed by ranging vacancies through the film, which is the so-called filament, whereas HRS is formed by repairing the vacancies only near the electrode interface.[2,12,13] This means that conductive filaments other than the neighborhood of the electrode interface remain without being repaired even in the HRS. Therefore, this is consistent with the fact that the writing region becomes dark whether it is in the HRS or the LRS in the SE image, assuming that a conductive region becomes dark in the SE image. Shima et al. performed Kelvin probe force microscopy and micro x-ray photoelectron spectroscopy measurements on the LRS of a CoO film that was written by the voltage application using C-AFM.[6] They reported that Fermi energy in CoO is pushed up because of reduction of CoO that causes defect-related energy levels in the band gap. Since it was reported that low secondary electron yield was related to a low work function,[14] our result also suggests that the C-AFM writing decreases a work function, which is consistent with Ref. 6. However, in Ref. 6, since a writing region is optically unidentifiable, the region excluding the region for which C-AFM writing will be performed is etched by using the photolithography to narrow down the writing region from the whole region to analyze the writing region by XPS. Therefore, it is worth noting that we obtained the result similar to that reported in Ref. 6 without the influence of the photolithography on the analyzed area of the sample.

IV. CONCLUSIONS

SEM and EPMA analyses on the C-AFM writing region revealed that the writing regions are distinguishable as dark areas in SE images. This enables one to specify the writing region without using complicated sample fabrication process to narrow down the writing regions such as the photolithography technique. In addition, EDS mapping analysis on the writing region suggested that the observed change in the contrast of the SE image is related to the intrinsic change in the electronic state of the NiO film, i.e., that the secondary electron yield is correlated to the physical properties of the film.

ACKNOWLEDGMENT

The authors thank H. Tanaka and H. Kasada for their experimental support.

REFERENCES

1. I.G. Baek, M.S. Lee, S. Seo, M.J. Lee, D.H. Seo, D-S. Suh, J.C. Park, S.O. Park, H.S. Kim, I.K. Yoo, U-In Chung, and J.T. Moon: Highly scalable non-volatile resistive memory using simple binary oxide driven by asymmetric unipolar voltage pulses. Electron Devices Meeting, IEDM Technical Digest (San Francisco, CA, 2004), p. 587.
2. K.M. Kim, B.J. Choi, and C.S. Hwang: Localized switching mechanism in resistive switching of atomic-layer-deposited TiO_2 thin films. *Appl. Phys. Lett.* **90**, 242906 (2007).
3. K. Kinoshita, T. Tamura, M. Aoki, Y. Sugiyama, and H. Tanaka: Lowering the switching current of resistance random-access memory using a hetero junction structure consisting of transition metal oxides. *Jpn. J. Appl. Phys.* **45**, L991 (2006).
4. J.F. Gibbons and W.E. Beadle: Switching properties of thin NiO films. *Solid-State Electron.* **7**, 785 (1964).
5. M-J. Lee, S. Han, S.H. Jeon, B.H. Park, S. Kang, S-E. Ahn, K.H. Kim, C.B. Lee, C.J. Kim, I-K. Yoo, D.H. Seo, X-S. Li, J-B. Park, J-H. Lee, and Y. Park: Electrical manipulation of nanofilaments in transition-metal oxides for resistance-based memory. *Nano Lett.* **9**, 1476 (2009).
6. H. Shima, F. Takano, H. Muramatsu, M. Yamazaki, H. Akinaga, and A. Kogure: Local chemical state change in Co–O resistance random-access memory. *Phys. Status Solidi* **2**, 99 (2008) (RRL).
7. C. Yoshida, K. Kinoshita, T. Yamasaki, and Y. Sugiyama: Direct observation of oxygen movement during resistance switching in NiO/Pt film. *Appl. Phys. Lett.* **93**, 042106 (2008).
8. K. Kinoshita, T. Okutani, H. Tanaka, T. Hinoki, K. Yazawa, K. Ohmi, and S. Kishida: Opposite bias polarity dependence of resistive switching in *n*-type Ga-doped ZnO and *p*-type NiO thin films. *Appl. Phys. Lett.* **96**, 143506 (2010).
9. J. Hsu, H. Lai, H. Lin, C. Chuang, and J. Huang: Fabrication of nickel oxide nanostructures by atomic force microscope nano-oxidation and wet etching. *J. Vac. Sci. Technol. B* **21**, 2599 (2003).
10. N. Hilleret, C. Scheuerlein, and M. Taborelli: The secondary-electron yield of air-exposed metal surfaces. *Appl. Phys., A Mater. Sci. Process.* **76**, 1085 (2003).
11. Y.B. Nian, J. Strozier, N.J. Wu, X. Chen, and A. Ignatiev: Evidence for an oxygen diffusion model for the electric pulse induced resistance change effect in transition-metal oxides. *Phys. Rev. Lett.* **98**, 146403 (2007).
12. K. Kinoshita, T. Tamura, M. Aoki, Y. Sugiyama, and H. Tanaka: Bias polarity dependent data retention of resistive random-access memory consisting of binary transition metal oxide. *Appl. Phys. Lett.* **89**, 103509 (2006).
13. I.H. Inoue, S. Yasuda, H. Akinaga, and H. Takagi: Nonpolar resistance switching of metal/binary-transition-metal oxides/metal sandwiches: Homogeneous/inhomogeneous transition of current distribution. *Phys. Rev. B* **77**, 035105 (2008).
14. M. Kudo, Y. Sakai, and T. Ichinokawa: Dependencies of secondary electron yields on work function for metals by electron and ion bombardment. *Appl. Phys. Lett.* **76**, 3475 (2000).

https://doi.org/10.1557/jmr.2010.57 Published online by Cambridge University Press